Journal of Applied Chemistry JAC
http://chemistry.journals.semnan.ac.ir

Starch-derived magnetic nanoparticles (Fe_3O_4@C-SO_3H): synthesis, characterization and its application on the preparation of dihydropyrano[c]chromenes, 2-Amino-3-cyano-4H-pyrans and 2-amino-4*H*-chromenes derivatives

Fatemeh Khorsi Damghani[1], Seied Ali Pourmousavi[1,*], Hamzeh Kiyani[2]
[1]*School of Chemistry, Damghan University, Damghan, Iran*
[2]*Institute of Biological Science, Damghan University, Damghan, Iran*

Article history:
Received:23/ Sep /2019
Received in revised form: 27/Nov/2019
Accepted: 29/Nov/2019

Abstract

In this study, a novel biomass and Starch-derived carbonaceous solid acid catalyst (Fe_3O_4@C-SO_3H) that has superparamagnetism with high acid density was successfully prepared for the first time by incomplete hydrothermal carbonization of Starch followed by Fe_3O_4 grafting and –SO_3H groups functionalization. The characterization of physicochemical properties of Fe_3O_4@C-SO_3H NPs was achieved by X-ray diffraction (XRD), Fourier-transform infrared spectra (FT-IR) and Field Emission scanning electron microscope (FESEM). The resulted catalyst contained -SO_3H, -COOH, and phenolic -OH groups and exhibited good catalytic activity for the one-pot synthesis of dihydropyrano[c]chromenes, 2-Amino-3-cyano-4H-pyrans and 2-amino-4*H*-chromenes derivatives (chromenes and pyrans) via multicomponent reactions. High catalytic activity and easy magnetical separation from the reaction mixture are two significant factors for evaluating the performance of Fe_3O_4@C-SO_3H nanoparticles in the organic transformations.

Keywords: Magnetic nanoparticles, Fe_3O_4@C-SO_3H, dihydropyrano[c]chromenes, Starch.

1.Introduction

In recent years, much attention has been focused on heterogeneous catalysts, since these catalysts can be recovered and reused several times after the reaction without loss of activity[1, 2].. Among the heterogeneous solid acid catalyst in organic synthesis, carbon base solid acids (CBSAs), which are important materials with many practical and research applications have been extensively studied [3].

On the other hand, the synthesis of magnetic sulfonated carbon nanoparticle indicating that the magnetism separation could be an efficient way to separate the catalyst from the reaction mixture [4]. The magnetic Fe_3O_4@C-SO_3H nanoparticle (MNPs) was widely studied and showed high catalytic activities in many chemical reactions. The enhanced activity of heterogeneous (MNPs) ascribed to the high stability of its acid sites, high density, carbon sheets hydrophobic

---

[*] **.Corresponding author:** at: School of Chemistry, Damghan University, Damghan, Iran, *Email: pourmousavi@du.ac.ir*

property, and the existence of $-SO_3H$ and $-COOH$ groups in its molecular structure. [5]. Many research nowadays focused on the production of these solid acid catalysts that are found to be recoverable and reusable which are eco-friendlier and greener than a catalyst in a liquid phase [6].

A multi-component reaction (or MCR), sometimes referred to as a "Multi-component Assembly Process" (or MCAP), is a chemical reaction where three or more compounds react to form a single product [7]. By definition, multicomponent reactions are those reactions whereby more than two reactants combine sequentially to give highly selective products that retain the majority of the atoms of the starting material.

The heterocyclic scaffold containing chromene and pyran represent a “privileged” structural motif well distributed in naturally occurring compounds [8-10]. Chromene moiety is present in naturally occurring compounds and interesting pharmaceutical materials. Chromenes and pyrans have attracted adult interest because they can exhibit a broad spectrum of significant biological activities such as antimicrobial [11], antifungal [12], antibacterial [13], antioxidant [14], antileishmanial [15], anticancer [16], and hypotensive [17]. Some of these compounds could also be applied as inhibitors [18, 19]. Fig. 1 represents a glimpse of some of 4H-chromenes which display strong biological activity including antibacterial, anticancer, and inhibitory.

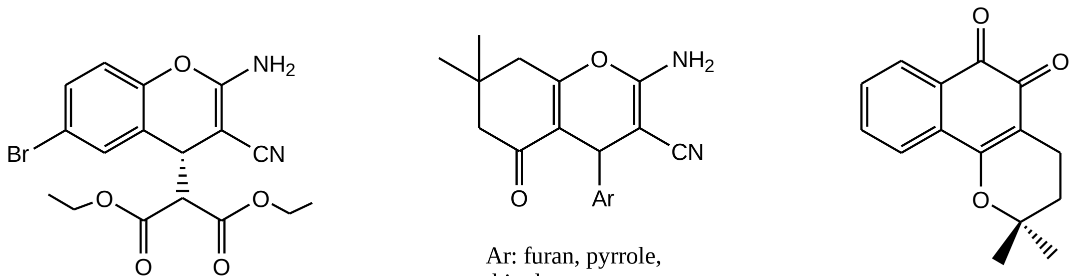

Ar: furan, pyrrole, thiophene

A: anticancer and Bcl-2 inhibitor

B: antibacterial and anticancer activity

C: β-lapachone- anticancer, anti-inflammatory, antibiotics

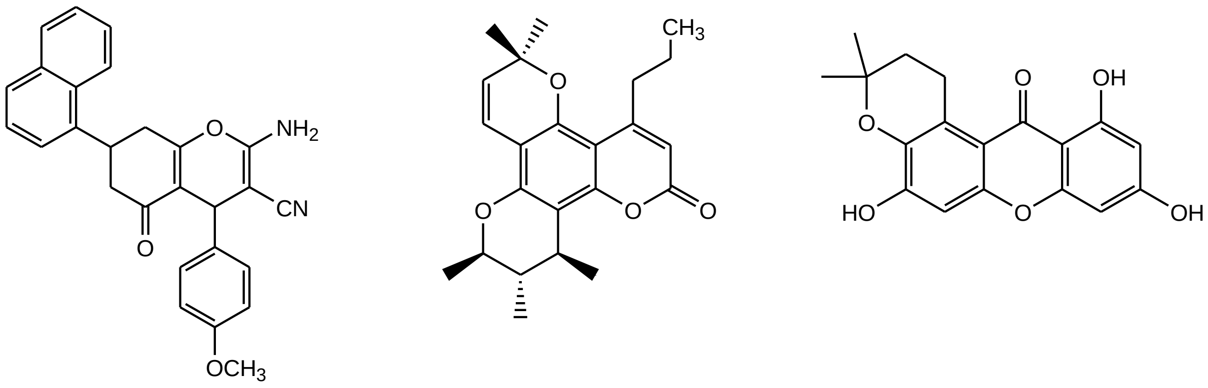

D: inhibitor of EAAT1

E: (+)-Calanolide A- anti-HIV

F: Hyperxanthone E- anti- tumor

Fig. 1. Selected examples of chromenes and pyrans derivatives with biological, inhibitory, and pharmacological activity.

Various types of homogeneous or heterogeneous catalysts have been applied to this heterocyclic system, such as silica nanoparticles [20], MgO [21], ferric hydrogen sulfate [22], meglumine [23], [bmim] OH [24, 25], DMAP, [26] SnO_2, [27] basic ionic liquid, [28] TBAB, [29, 30] DBU, [31] diammonium hydrogen phosphate, [32] nano ZnO, [33] (S) proline [34]. Although these procedures reported by others find certain merits of their own, however, many of these approaches suffer from some drawbacks including prolonged reaction times, tedious workup procedures, expensive catalyst/reagents, high catalytic loading; and as well as the requirement of special apparatus. Thus, a search for more general, simple, efficient, feasible, and high yielding routes to this class of the organic molecules remains a valid exercise.

In this work, we developed a rapid and efficient protocol for the synthesis of some derivatives of chromenes and pyrans using Fe_3O_4@C-SO_3H as green and reusable catalysts.

2. materials and methods

All chemicals were used as received without further purification. Iron (III) chloride hexahydrate ($FeCl_3\cdot 6H_2O$, 99.0%), Iron (II) Sulfate Heptahydrate ($FeSO_4$, $7H_2O$, 99.0%) and other chemical materials were purchased from Fluka and Merck Companies. Products were characterized by comparison of their physical data, IR and ^{1}H NMR and ^{13}C NMR spectra of known samples. All ^{1}H-NMR and ^{13}C NMR spectra were recorded at 500 MHz in DMSO relative to TMS (0.00 ppm). IR spectra were recorded on Perkin-Elmer Spectrum RXI FT-IR spectrophotometer. X-ray diffraction (XRD) patterns of samples were taken on a Philips X-ray diffract meter Model PW 1840. The particle morphology was examined by FESEM (Philips XL30 scanning electron microscope).

3. Experimental

3.1.1. Preparation of the Fe_3O_4 (MNPs)

Fe_3O_4 MNPs were synthesized by coprecipitation method [35]. Typically, 2 gr of $FeCl_3\cdot 6H_2O$ and 1 gr of $FeSO_4\cdot 7H_2O$ were dissolved in 250 mL of deionize water at 60 °C. Then, NaOH (2 M) solution was added to keep the pH between 10 and 11. After being rapidly stirred for 6 h, the magnetic core was obtained by the magnetic attraction and washed with water and dried at 60 °C in vacuum for 4h.

3.1.2. Synthesis of the carbon-based solid acid (C–SO_3H)

The Sulfuric acid (10 ml) was mixed with Starch (5 g). Then, the mixture was transferred into the autoclave at 180 ^{0}C for 24 h. The solid black product was washed with water. The carbon-based solid acid was obtained after drying at 80 ^{0}C.

3.1.3. Synthesis of the Fe_3O_4@C–SO_3H MNPs

For a typical procedure, magnetic Fe_3O_4 nanoparticles MNPs (3 g) and carbon-based solid acid (C–SO_3H), (1 g) were mixed with 80 mL water in a flask under vigorous stirring in an oil bath at 100 °C. After evaporation of water, the mixture was transferred into a 100 mL Teflon-sealed autoclave. The autoclave was kept at 180 °C for 6 h before cooled naturally the carbon Intermediate were separated by a magnet, and washed with deionized water and ethanol several times to neutral solution, and dried in an oven.

3.2 Synthesis of chromene by β-Naphthol, Dimedone or 4-hydroxycoumarin using Fe_3O_4@C–SO_3H

A mixture of Aryl aldehyde (1 mmol), β-Naphthol, Dimedone or 4-hydroxycoumarin compound (1 mmol), Malononitrile (1.2 mmol, 0.0726 g), Fe_3O_4@C–SO_3H catalyst (0.03 g) and 5 mL water were taken in a round-bottom flask and stirred and heated at 60 ^{0}C for a time (monitored by TLC). After satisfactory completion of the reaction and cooling, the catalyst was collected by an external magnet, and the reaction mixture was washed with ethanol. The organic layer was concentrated under reduced pressure and then the product so obtained was recrystallized from ethanol to afford the pure product.

3.2.1. 3-amino-1- (4-chlorophenyl) -1H-benzo [f] chroman-2-carbonitrile (Table 3: entry e).

Cream powder, m.p. 205-208 °C; IR (potassium bromide): (υ_{max}, cm^{-1}): 3411, 3326, 2193, 1643, 1591, 1488, 1404, 1234, 1093; δH (ppm): 4.41 (s, 1H), 4.55 (s, 2H, NH_2), 7.30 (m, 1H), 7.37 (t, 1H, J = 6.7), 7.52 (t, 1H, J = 6.1), 7.54 (d, 1H, J = 7.7), 7.85 (m, 1H), 8.0 (m, 2H), 8.52 (d, 1H, J = 6.7), 8.62 (d, 2H, J = 8.3).

3.2.2 2-amino-5-oxo-4- (3, 4 di-methoxyphenyl) -5, 4-dihydropriano [3, c-2] - chromene -3-carbonitrile (Table 3: entry j)

Yellow powder, m.p. 230-232 °C; IR (potassium bromide) (υ_{max}, cm^{-1}): 3367, 1668, 1608, 1587, 1484 cm^{-1}. δH (ppm): 3.93 (s, 3H), 3.98 (s, 3H), 4.37 (s, 1H), 4.49 (s, 2H, NH), 7.29 (t, 1H, J = 7.1 Hz), 7.37 (t, 1H, J = 7.5 Hz), 7.53 (t, 1H, J = 8.0 Hz), 7.58 (d, 1H, J = 7.3 Hz), 7.84 (s, 1H), 7.98 (d, 1H, J = 7.5 Hz), 8.09 (d, 1H, J = 8.1 Hz).

3.2.3 2-amino-3-cyano-7, 8-dihydro-4- (4-hydroxyphenyl) -H4-chroman -5 (6) –one (Table 4: entry n)

White powder, m.p. 226-228 °C; IR (potassium bromide): (υ_{max}, cm^{-1}): 3430, 3110, 3041, 1706, 1606, 1519, 1309, 1201, 1103, 941; δH (ppm): 1.05 (s. 3H), 1.12 (s. 3H), 2.23 (d, *J* = 8.3 Hz, 2H), 2.45 (d, *J* = 8.4 Hz, 2H), 4.37 (s, 1H), 4.49 (s, 2H, NH), 4.89 (s, 1H, OH), 6.75 (d, *J* = 8.5 Hz, 2H), 7.12 (d, *J* = 8.4 Hz, 2H).

4. Result and Discussion

The synthetic procedure for the Fe_3O_4@C–SO_3H solid acid catalysts is shown in Scheme 1.

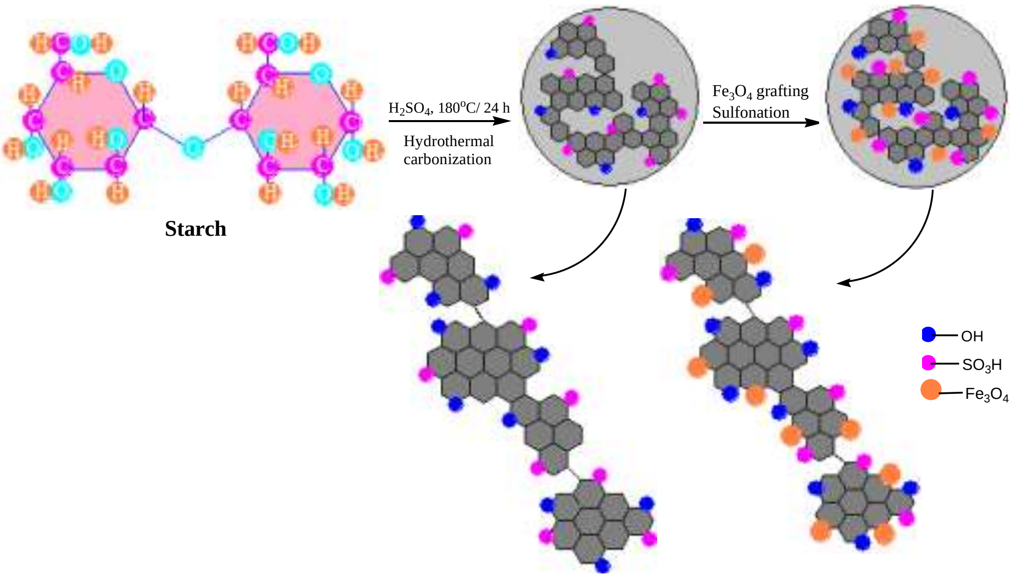

Scheme 1. The synthetic route of the magnetic carbon-based solid acid.

Firstly, the Fe_3O_4 was prepared according to the reported method [35] and carbon-based solid acid (C–SO_3H) was synthesis by the reaction of a mixture of Sulfuric acid and Starch in a 100 mL Teflon-Lined Autoclave Reactor. Then, Fe_3O_4 MNPs and carbon-based solid acid (C–SO_3H), were mixed and the mixture was transferred into a 100 mL Teflon-sealed autoclave. The resulted sulfonic acid-functionalized magnetic nanoparticles were denoted as Fe_3O_4@C-SO_3H.

Consequently, as-synthesized Fe_3O_4@C-SO_3H was used the solid acid catalyst in the preparation of Heterocyclic compounds with high efficiency under mild conditions. One of the advantages of this nanocatalyst is that this catalyst can be separated by an external magnet (0.2 T), and be then reused several times. The separation of the catalyst by an external magnet was shown in Fig. 1.

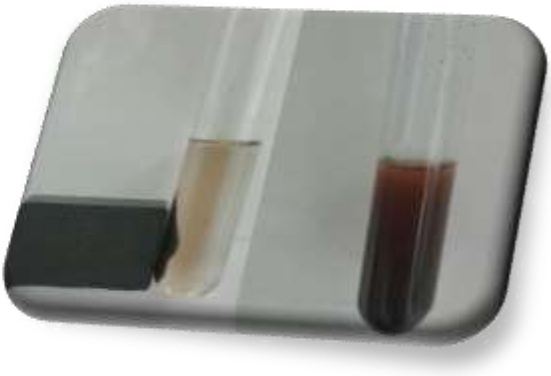

Fig. 1 The separation of catalyst by an external magnet

The total acid density and the sulphonic acid density of Fe_3O_4@C–SO_3H were obtained based on the acid-base titration. To determine total acid density, the catalyst sample (0.04 g) was mixed with NaOH solution (10 mL, 0.01 mol/L) and was stirred for 2 h at room temperature for neutralizing the surface acidity of catalyst. The consumed base concentration was back-titrated by HCl solution (0.01mol/L) with phenolphthalein as the indicator [36]. The acid loading of the sulfonic group functionalized Fe_3O_4@C MNPs was determined by an ion exchange reaction of H^+ by Sodium cation and then titration of released H^+ ion [37]. The ion exchange reaction for the catalysts was achieved by treating 0.03 g of the sample with 6 ml of a NaCl solution (2 N) for 24 h at room temperature. The catalysts were separated using an external magnet, and the NaCl solution was decanted and saved. The same procedure was repeated to ensure that all the protons have been exchanged completely. Then, two drops of a phenolphthalein solution were added to the NaCl solution. The solution was titrated to neutrality using a 0.01 M NaOH solution to determine the loading of acid sites of the catalyst MNPs. The results of titration of the solid acid was shown in Table 1.

Table 1.The total acid density of Starch -derived catalyst

Entry	sulfuric acid (ml)	Starch (g)	Acid site density (mmol/g)	
			Total	SO_3H
1	10	1	8.67	1.37

Fig. 2 shows representative X-ray powder diffraction (XRD) patterns of nanoparticle catalyst. As shown in Fig. 2, characteristic diffraction peaks were observed at 30.3°, 35.4°, 43.1°, 53.4°, 56.9° and 62.5°, which were assigned to the (220), (311), (400), (422), (511), and (440) lattice planes of Fe_3O_4 , respectively. After a series of treatments including functionalization of Fe_3O_4 MNPs with C–SO_3H Solid Acid, the magnetite nanoparticles were stable, as revealed by the XRD

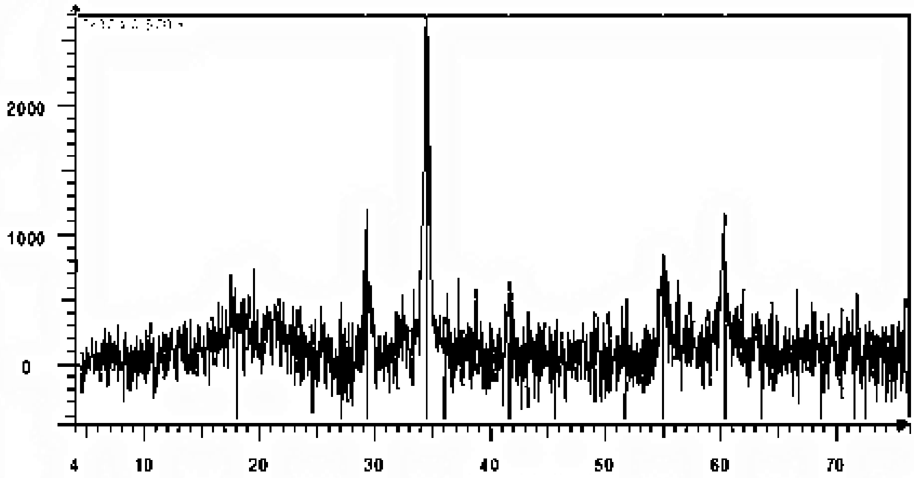

Fig. 2: XRD spectra of the catalyst Fe_3O_4@C–SO_3H

The components of the nanocatalyst were analysis using Field Emission Scanning Electron Microscope (FESEM) in Fig. 3 and Fig. 4. FESEM spectrums in Fig. 3 show that C–SO_3H nanoparticles are nearly spherical with Nano dimension ranging from 28 to 36 nm in size and smoother surface. FESEM spectrums in Fig. 4 show that conditions in which aggregation of uniform particles of 27-40 nm in size was observed. According to Fig. 3 and 4 to form the core-shell structures, the concentration of the magnetic core and carbohydrate should be controlled carefully, which resulted in low solid yield [38]. No significant difference in morphology was observed among the prepared catalyst after a series of treatments including magnetite nanoparticles by the FESEM analysis.

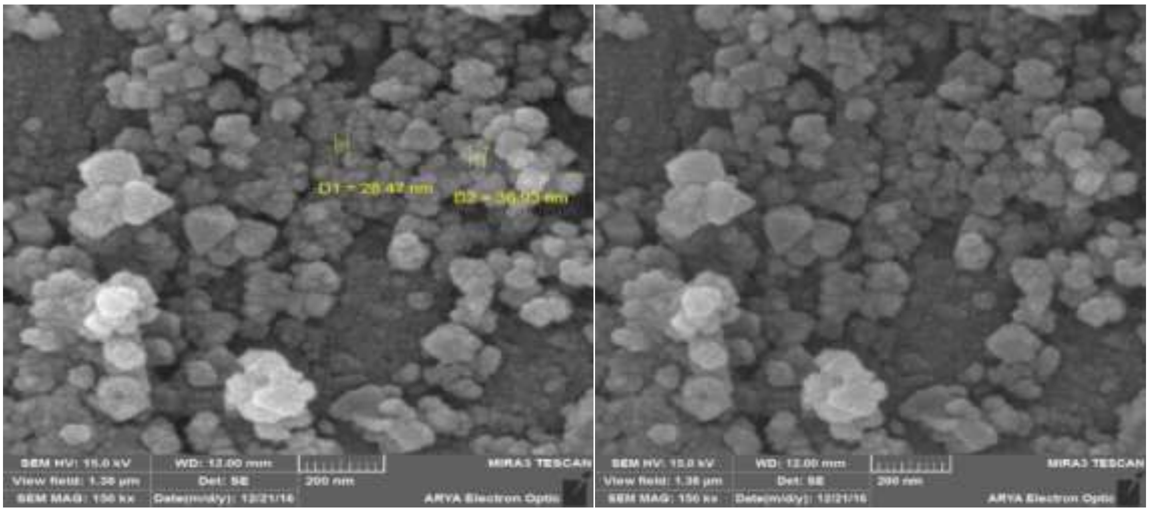

Fig. 3. FESEM images of the C–SO_3H

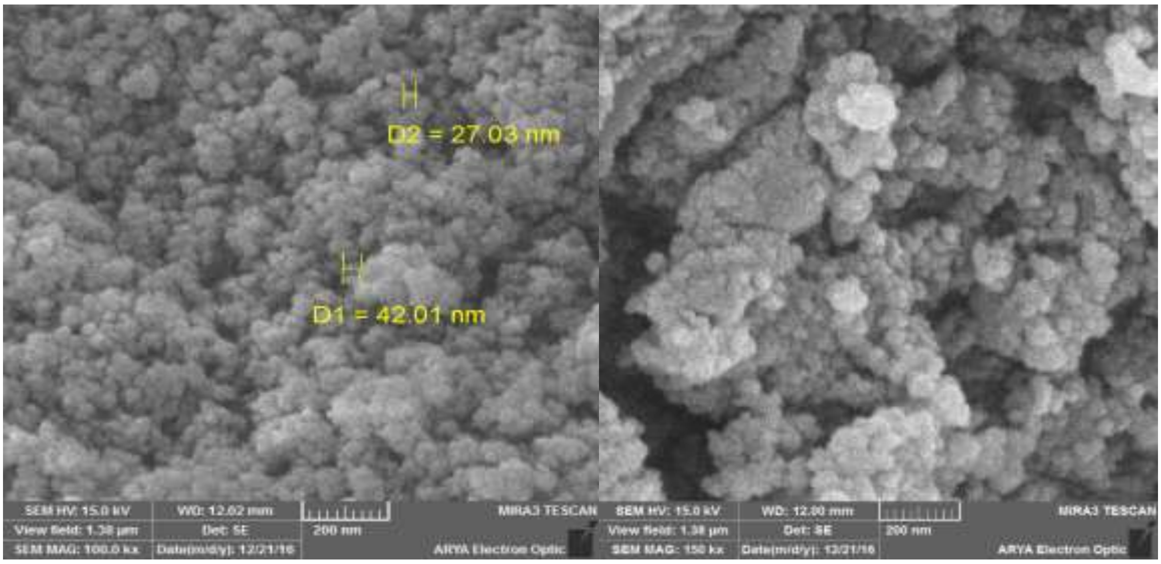

Fig. 4. FESEM images of the catalyst Fe_3O_4@C–SO_3H

FT-IR spectrum (Fig. 5) showed characteristic peaks at 1026 cm^{-1} and 1174 cm^{-1} which are attributed to O=S=O stretching vibrations in -SO_3H groups and peak at 1127 cm^{-1} for SO_3H stretching. This indicates that the sulfonic acid groups have been successively incorporated on the catalyst surface. The Peaks at 1642 cm^{-1} ascribed to C=O stretching vibration of the –COOH group. The Bands due to O-H stretching were observed at 3429 cm^{-1}.

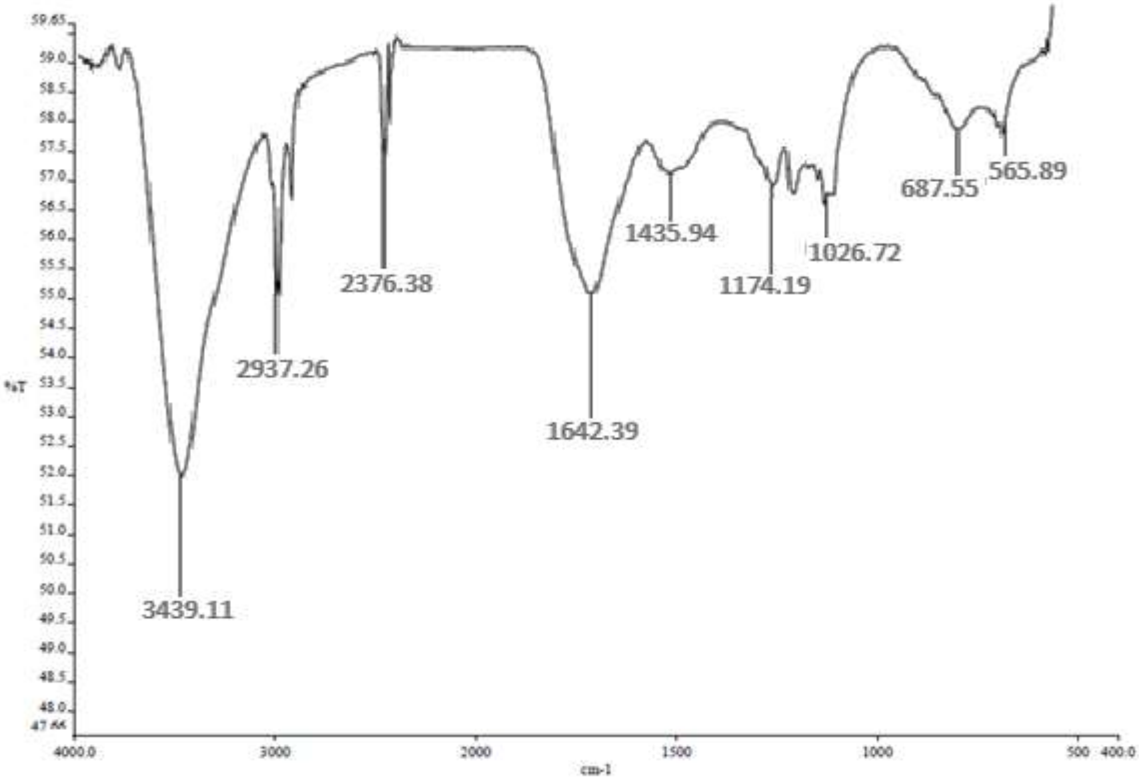

Fig. 5. FT-IR spectrum of Nano catalyst**.**

The catalyst was examined by TGA analysis as shown in Fig. 6. The decomposition pattern shows two stages of weight loss for the $Fe_3O_4@C–SO_3H$ sample. First stage was starting from 100 to 200 ^{O}C due to lost of water (around 10 wt. %). The second stage shows another of weight loss (circa 50 wt. %) starting from 300 to 800 ^{O}C that indicated the decomposition of carboxylic group, COOH and sulfonic, $C-O-SO_3H$ functional groups for the $Fe_3O_4@C–SO_3H$ catalyst.

Fig. 6. TGA curve of superparamagnetic carbonaceous material functionalized with sulfonic acid groups ($Fe_3O_4@C–SO_3H$).

After characterization of the solid acid catalyst, the catalytic activity of core-shell magnetic nanoparticles MNPs was tested in the preparation of some heterocyclic derivatives. To investigate the catalytic performance of the $Fe_3O_4@C-SO_3H$ core-shell magnetic nanoparticles MNPs, the synthesis of chromene and pyran derivatives was chosen.

In this study, $Fe_3O_4@C-SO_3H$ was used to catalyze the condensation of aldehyde, malononitrile, and β-naphthol, Dimedone or 4-hydroxycoumarin to give of chromene derivatives. (Scheme 2)

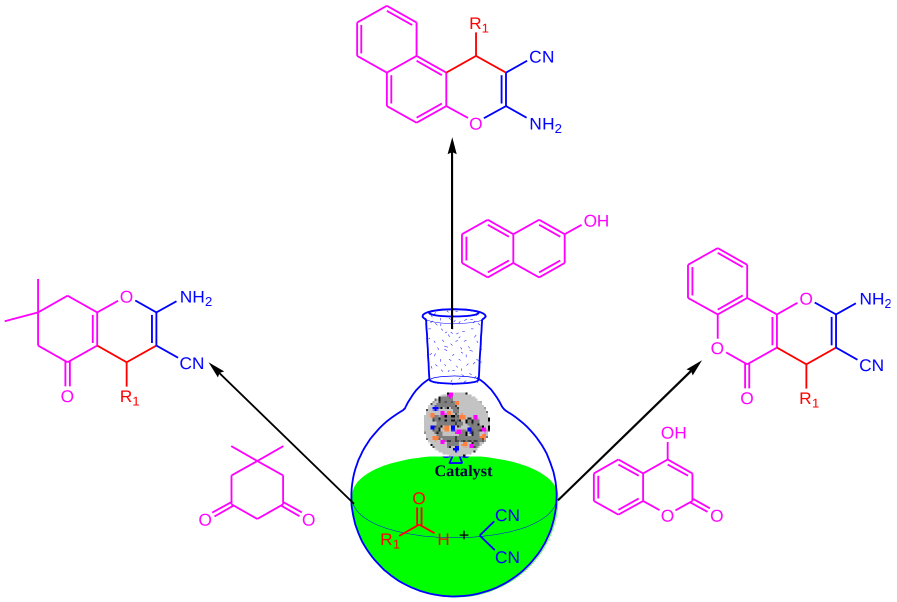

Scheme 2: Synthesis of chromene and pyran derivatives by condensation of aldehyde, malononitrile and β-naphthol, Dimedone or 4-hydroxycoumarin using Fe_3O_4@C-SO_3H

For optimizing the experimental conditions, the reaction between malononitrile, benzaldehyde, and β-naphthol, Dimedone or 4-hydroxycoumarin in the presence of Fe_3O_4@C-SO_3H was considered as a model reaction (Scheme 3).

This condensation reaction was studied in various solvents at different temperatures and with differing amounts of catalysts.

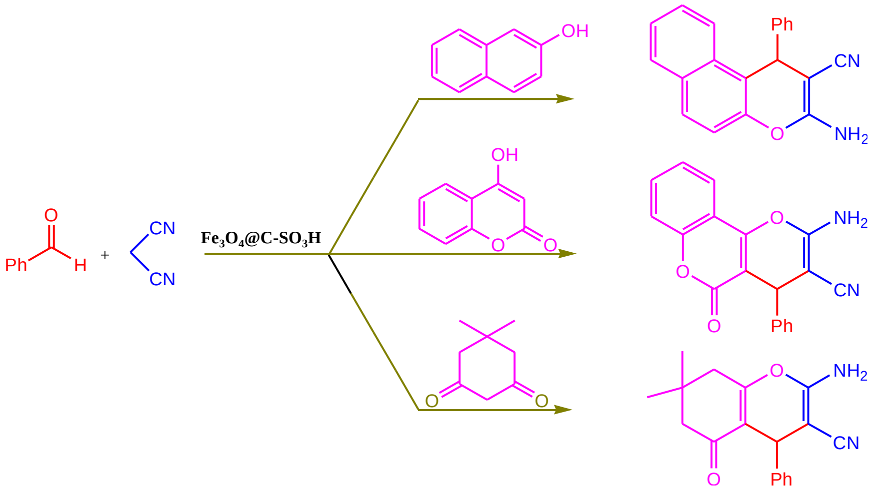

Scheme 3: model reaction for the synthesis of chromenes and pyrans.

Table 2. Optimization of the reaction conditions for the synthesis of chromene and pyran [a]

Entry		Catalyst. (g)	T. (°C)	Solvent	Time (m)	Yield (%)[b]
1	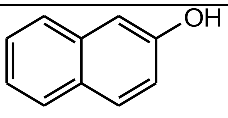	-	100	-	180	-
2	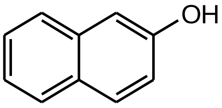	0.01	100	-	180	40
3	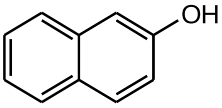	0.02	100	-	180	55
4	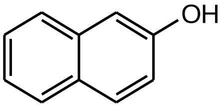	0.03	100	-	180	70
5	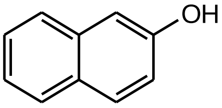	0.03	Reflux	H_2O	160	85
6	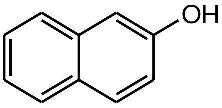	0.03	80	H_2O	160	85
7	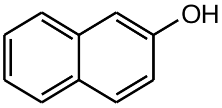	0.03	60	H_2O	160	85
8	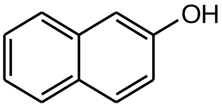	0.03	40	H_2O	160	65
9	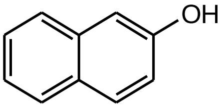	0.03	Reflux	n-hexane	190	10
10	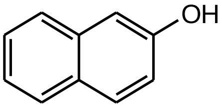	0.03	Reflux	Ethyl acetate	180	30
11	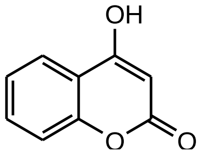	-	100	-	240	-
12	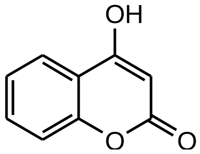	0.01	100	-	240	5
13	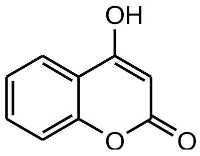	0.02	100	-	240	30

14	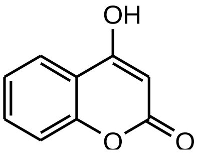	0.03	100	-	240	55
15	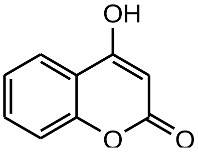	0.03	Reflux	H_2O	200	80
16	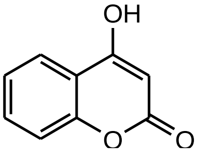	0.03	80	H_2O	200	80
17	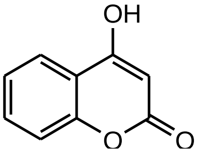	0.03	60	H_2O	200	80
18	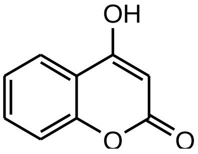	0.03	40	H_2O	200	50
19	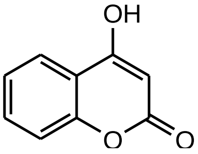	0.03	Reflux	n-hexane	260	5
20	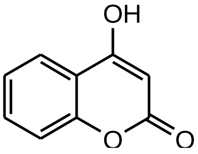	0.03	Reflux	- Ethyl acetate	240	15
21	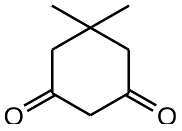	-	100	-	120	-
22	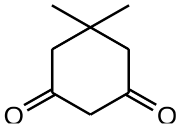	0.01	100	-	60	30
23	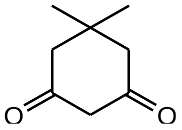	0.02	100	-	60	60
24	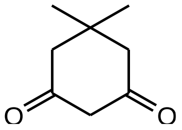	0.03	100	-	60	80
25	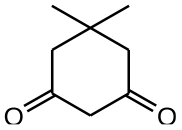	0.03	Reflux	H_2O	40	87

26	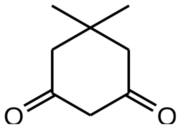	0.03	80	H_2O	40	87
27	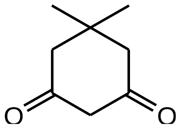	0.03	60	H_2O	40	87
28	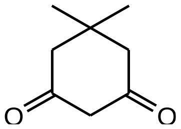	0.03	40	H_2O	40	60
29	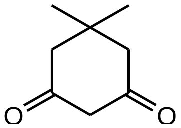	0.03	Reflux	n-hexane	120	5
30	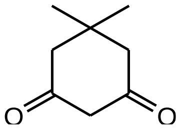	0.03	Reflux	Ethyl acetate	240	20

[a] Reaction conditions: benzaldehyde (1 mmol), malononitrile (1 mmol), β-naphthol, Dimedone or 4-hydroxycoumarin (1 mmol), and Fe_3O_4@C-SO_3H under conditions. [b] Isolate yield.

The best conditions were found to be 0.03 g catalyst at 60 °C in H_2O (Table 2, entry 7, 17 and 27).

To see the applicability of this reaction, various aromatic aldehydes were used according to the Scheme 4 and the results of this study are presented in Table 3.

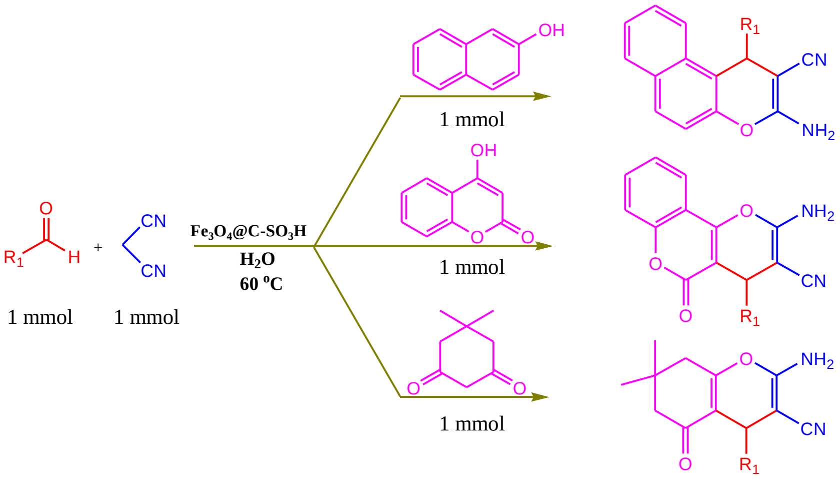

Scheme 4. Synthesis of chromene and pyran derivatives condensation reaction.

Table 3: Preparation of chromene and pyran derivatives using $Fe_3O_4@C\text{-}SO_3H$.

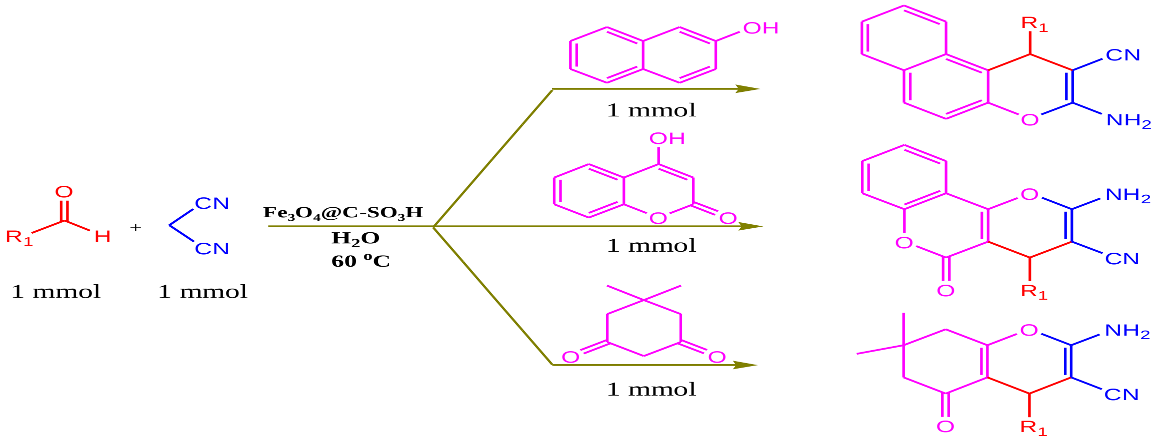

Entry	R1	Enole or Naphtole	Time (m)	Yield^a (%)	M.p.°C	Ref
A	C_6H_5	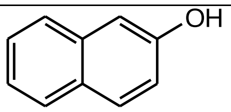	160	85	277-280	277-280 [39]
B	$4\text{-}NO_2C_6H_4$	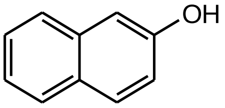	120	90	199-200	185-186 [39]
C	$4\text{-}OHC_6H_4$	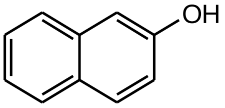	190	70	223-226	234-236 [39]
D	$3,4\text{-}(CH_3O)_2C_6H_3$	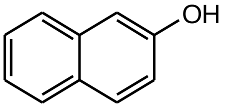	210	75	150-152	--------
E	$4\text{-}ClC_6H_4$	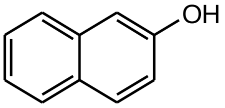	130	80	200-202	208-210 [39]
F	C_6H_5	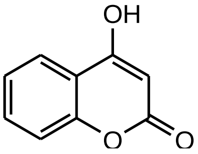	200	80	254-255	254-256 [40]
G	$4\text{-}NO_2C_6H_4$	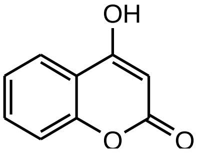	150	87	253-256	258-260 [40]
H	$4\text{-}OHC_6H_4$	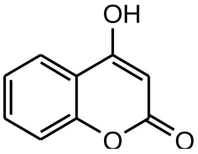	230	65	258-261	262-264 [41]
J	$3,4\text{-}(CH_3O)_2C_6H_3$	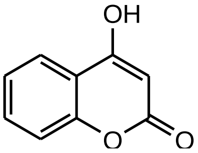	240	60	249-250	268-269 [41]

K	4-ClC_6H_4	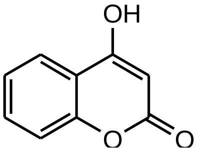	100	85	260-263	262-264 [42]
L	C_6H_5	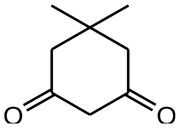	40	80	286-288	286-288 [43]
M	4-$NO_2C_6H_4$	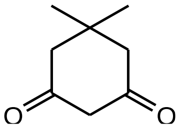	30	80	287-289	287-289 [44]
N	4-OHC_6H_4	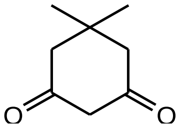	60	75	214-216	213-214 [44]
P	3,4-$(CH_3O)_2C_6H_3$	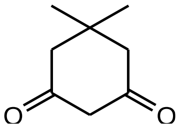	70	60	204-206	214-216 [45]
N	4-ClC_6H_4	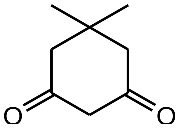	30	85	213-214	212-214 [45]

^{a}yield of isolated pure products.

5. Recycling of the catalyst

The magnetic property of the solid acid is an emerging solution for overcoming separation problems. Therefore, determining the recyclability of a catalyst is significant to evaluate its efficiency based on economic and environmental factors. As shown in Figure 1a, the used Fe_3O_4@C–SO_3H catalyst could be separated from the resulting reaction mixture easily via applying an external magnetic field. After separation, the catalyst was repeatedly washed with water, dried, and then used in a subsequent experiment at identical reaction conditions and its recycled catalytic activities for Chromenes production are shown in Fig. 7. It can be seen that the Fe_3O_4@C–SO_3H catalyst remained active for each recycles run. Decreasing the yield is probably related to slight reduction in the catalytic activity of the catalyst or decreasing the amount of catalyst recovery which is attributed to the handling.

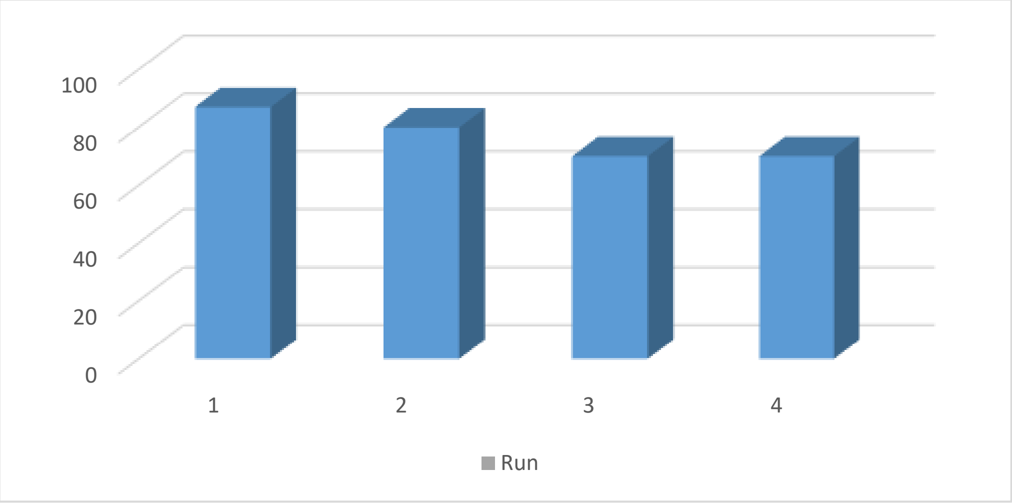

Fig. 7: Recycled catalytic activities of the Fe_3O_4@C–SO_3H catalyst for Chromene production.

5. Conclusion

In Conclusions, the present study clearly showed that the starch-derived solid acid, prepared through sulfonation of incompletely carbonized starch in the presence of Fe_3O_4 nanoparticles, is the non-toxic, inexpensive and promising eco-friendly catalyst. This catalyst also manifested very excellent operational stability. Also, the Fe_3O_4 core makes the catalyst to be easily recovered by an externally applied magnetic field. Chromene and pyran derivatives are successfully synthesized using Fe_3O_4@C-SO_3H respectively. The mildness of the conversion, experimental simplicity, compatibility with various functional groups, excellent yields, short reaction times and the easy workup procedure makes this protocol an attractive and user-friendly alternate method for the synthesis of substituted chromenes.

Acknowledgments:

The authors are thankful to Damghan University Research Council for the partial support of the work.

References

[1] S. Kang, J. Ye and J. Chang, *Int. Rev. Chem. Eng, (IRECHE).* **5** (2013) 133.

[2] C. Zhang, H. Wang, F. Liu, L. Wang and H. He, *Cellulose.* **20**, (2013) 127.

[3]. D. Lai, L. Deng, Q. Guo and Y. Fu, *Energy Environ Sci*. **4** (2011) 3552.

[4]. R. Rinaldi, R. Palkovits and F. Schuth, *Angew Chem Int Ed Engl.* **47** (2008) 8047.

[5]. X. Zheng, S. Luo, L. Zhang and JP. Cheng, *Green Chem.* ***11*** *(2012) 455.*

[6]. DJ. Ramon and M. Yus, *Angew Chem Int Ed Engl.* **44** (2005) 1602.

[7]. W. R. Armstrong, P. A. Combs, A. p. Tempest, S. D. Brown and A. K. Thomas, *Chem. Res.* **29** (1996) 123.

[8]. G. Feuer, *Progress in Medicinal Chemistry*, G. P. Ellis, G. P. West, Eds. North-Holland Publishing Company: New York, **10** (1974) 85.

[9]. F. M. Dean, *Nature.* **200** (1963) 176.

[10]. A. Goel and V. J Ram, *Tetrahedron.* **65** (2009) 7865.

[11]. H.G. Kathrotiya and M.P. Patel, *Med. Chem. Res.* **21** (2012) 3406.

[12]. L. Alvey, S. Prado, B. Saint-Joanis, S. Michel, M. Koch, S.T. Cole and F. Tillequin, Y.L. Janin, *Eur. J. Med. Chem.* **44** (2009) 2497.

[13]. D. Kumar, V.B. Reddy, S. Sharad, U. Dube and S. Kapur, *Eur. J. Med. Chem.* **44** (2009) 3805.

[14]. T. Symeonidis, M. Chamilos, D.J. Hadjipavlou-Litina, M. Kallitsakis and K.E.

Litinas, *Bioorg. Med. Chem. Lett*. **19** (2009) 1139.

[15]. T. Narender and S. Shweta, *Bioorg. Med. Chem. Lett.* **19** (2009) 3913.

[16]. P.K. Paliwal, S.R. Jetti and S. Jain, *Med. Chem. Res.* **22** (2013) 2984.

[17]. S.X. Cai, J. Drewe and W. Kemnitzer, *Med. Chem.* **9** (2009) 437.

[18]. T.H.V. Huynh, B. Abrahamsen, K.K. Madsen, A. Gonzalez- Franquesa, A.A. Jensen and L. Bunch, *Bioorg. Med. Chem.* **20** (2012) 6831.

[19]. J.L. Wang, D.X. Liu, Z.J. Zhang, S.M. Shan, X.B. Han, S.M. Srinivasula, C.M. Croce, E.S. Alnemri and Z.W. Huang, *Proc. Natl. Acad. Sci. U.S.A.* **97** (2000) 7124.

[20]. S. Banerjee, A. Horn, A. Khatri and G. Sereda, *Tetrahedr. Lett.* **52** (2011) 1878.

[21]. D. Kumar, V.B. Reddy, S. Sharad, U. Dube and S. Kapur, *Eur. J. Med. Chem.* **44** (2009) 3805.

[22]. H. Eshghi, S. Damavandi and G.H. Zohuri, *Synth. React. Inorg. Met.* **41** (2011) 1067.

[23]. R.-Y. Guo, Z.-M. An, L.-P. Mo, R.-Z. Wang, H.-X. Liu, S.-X. Wang and Z.-H. Zhang, *ACS Com. Sci.* **15** (2013) 557.

[24]. K. Gong, H.-L. Wang, J. Luo and Z.-L. Liu, *J. Heterocycl. Chem.* **46** (2009) 1145.

[25]. J.M. Khurana and A. Chaudhary, *Green Chem. Lett. Rev.* **5** (2012) 633.

[26]. A. T. Khan, M. Lal, S. Ali and Md. M Khan, *Tetrahedron Lett.* **52** (2011) 5327.

[27]. Y. Sarrafi, E. Mehrasbi, A. Vahid and M. Tajbakhsh, *Chin. J. Catal.* **33** (2012) 1486.

[28]. K. Gong, H. L. Wang, J. Luo and Z. L. Liu, *J. Heterocycl. Chem.* **46** (2009) 1145.

[29]. S. Gurumurthi, V. Sundari and R. Valliappan, *E-J. Chem.* **6** (2009) 466−472.

[30]. J. M. Khurana and S. Kumar, *Tetrahedron Lett.* **50** (2009) 4125.

[31]. J. M Khurana, B. Nand and P. Saluja, *Tetrahedron.* **66** (2010) 5637.

[32]. S. Balalaie, M. Bararjanian, M. Sheikh-Ahmadi, S. Hekmat and P. Salehi, *Synth. Commun.* **37** (2007) 1097.

[33]. S. Paul, P .Bhattacharyya and A. R. Das, *Tetrahedron Lett.* **52** (2011) 4636.

[34]. S. Balalaielalaie, M. Bararjanian, A. M. Amani and B. Movassagh, *Synlett.* **2** (2006) 0263.

[35]. X. Liu, Z. Zhong, Y. Tang and B. Liang, *J. Nanomat.* **10** (2013) 1155.

[36]. WS. Mok, MJ. Antal and G. Varhergyi, *Ind Eng Chem Res.* **31** (1992) 94.

[37]. K. Nakajima and M. Hara, *ACS Catal.* **2** (2012) 1296.

[38]. Y. Lunxiang and L. Jurgen, *Chem. Rev.* **107** (2007) 133.

[39]. V. P. Pagore, S. U. Tekale, B.D. Rupnar and R. P. Pawar, *J. Chem. Pharm. Res.* **7** (2015) 1057.

[40]. G. Brahmachari and B. Banerjee. *ACS Sustainable Chem. Eng.* **2** (2014) 411.

[41]. S. Jain, D. Rajguru, B. S. Keshwal and A.D. Acharya, *ISRN Org. Chem.* **2013** (2013) 5

[42]. B.V. Shitole, N. V. Shitole and G. K. Kakde, *J. Chem.* **9** (2017) 131.

[43]. M. G. Dekamin, M. Eslami and A. Maleki, *Tetrahedron.* **69** (2013) 1074.

[44]. S. M. Vahdat1, M. Khavarpour and F. Mohanazadeh. *J. Appl. Chem.* **9** (2015) 41.

[45]. H. Kiyani and F. Ghorbani. *J. Saudi Chem. Soc.*. **18** (2014), 689.